

PAPER • OPEN ACCESS

In situ ac Stark shift detection in light storage spectroscopy

To cite this article: D Palani *et al* 2021 *J. Phys. B: At. Mol. Opt. Phys.* **54** 165402

View the [article online](#) for updates and enhancements.

You may also like

- [Ultracold polar molecules as qubits](#)
Rahul Sawant, Jacob A Blackmore, Philip D Gregory *et al.*
- [Optimal superadiabatic population transfer and gates by dynamical phase corrections](#)
A Vepsäläinen, S Danilin and G S Paraoanu
- [Relationship measurement between ac-Stark shift of \$^{40}\text{Ca}^+\$ clock transition and laser polarization direction](#)
Hong-Fang Song, , Shao-Long Chen *et al.*

In situ ac Stark shift detection in light storage spectroscopy

D Palani¹ , D Hoenig¹  and L Karpa^{1,2,*} 

¹ Albert-Ludwigs-Universität Freiburg, Physikalisches Institut, 79104 Freiburg, Germany

² Leibniz Universität Hannover, Institut für Quantenoptik, 30167 Hannover, Germany

E-mail: karpa@iqo.uni-hannover.de

Received 26 May 2021, revised 27 July 2021

Accepted for publication 20 August 2021

Published 9 September 2021



Abstract

We report on a method for measuring ac Stark shifts observed in stored light experiments while simultaneously determining the energetic splitting between the electronic ground states involved in the two-photon transition. To this end, we make use of the frequency matching effect in light storage spectroscopy. We find a linear dependence on the intensity of the control field applied during the retrieval phase of the experiment. At the same time, we observe that the light shift is insensitive to the intensity of the signal field which is in contrast to continuously operated electromagnetically induced transparency (EIT) or coherent population trapping (CPT) experiments, where the light shifts induced by all participating optical fields have to be taken into account. Our results may be of importance for future precision measurements in addition to or in combination with current EIT and CPT-type devices which are largely compatible with our approach and could benefit from the inherent robustness regarding operational conditions, shape of the resonances or intensity fluctuations in the signal field.

Keywords: light–matter interaction, coherent control, atomic clocks

(Some figures may appear in colour only in the online journal)


1. Introduction

The coherent interaction of optical fields with multilevel systems gives rise to interesting phenomena such as coherent population trapping (CPT) [1, 2] and electromagnetically induced transparency (EIT) [3, 4]. These closely related effects arise from the emergence of non-interacting states comprised of coherent superpositions of electronic ground states which in the ideal case have no contribution of the excited state. Such dark states are responsible for the occurrence of narrow transmission peaks (EIT) [5] in otherwise opaque media and the associated drastically reduced group velocities known as slow light [6–8]. These phenomena have fostered applications in magnetometry [9–11] and atomic clocks [11] where the ac Stark shift induced by all optical fields on the energy levels

of the interacting media is a major concern met with continuously developed elaborate measurement schemes to mitigate its impact [11–18]. With this progress, CPT-based clocks now reach a stability on the order of one part in 10^{15} , but a method providing inherent insensitivity to light field-induced shifts and other detrimental effects such as line-shape-asymmetry-induced (LAI) shifts [19] would be advantageous.

Such experiments typically involve the coupling of two resonant optical fields, a strong control field, and a weaker signal field, to effective Λ -type three-level atomic systems. Dynamic manipulation of the properties of the light fields allows for a reduction of the associated group velocity to zero and subsequent reversal of this process at a later time, a procedure referred to as light storage [20–22]. It was shown that upon retrieval of a previously stored light pulse, the difference frequency between the signal and control fields matches the energy splitting of the ground states in the probed three-level system [23]. This effect known as frequency matching which can be understood within the framework of the polariton picture of EIT occurs regardless of the initial two-photon detuning

* Author to whom any correspondence should be addressed.

 Original content from this work may be used under the terms of the [Creative Commons Attribution 4.0 licence](https://creativecommons.org/licenses/by/4.0/). Any further distribution of this work must maintain attribution to the author(s) and the title of the work, journal citation and DOI.

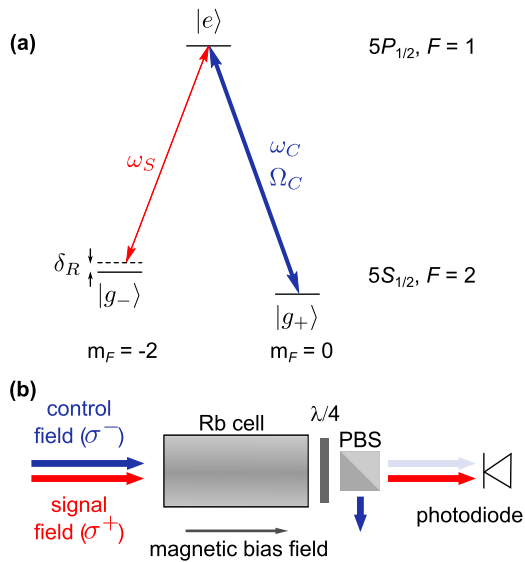


Figure 1. (a) Simplified level scheme of the ^{87}Rb D1 line. The electronic states comprising the idealized three-level Λ system are addressed by two optical fields, a circularly polarized (σ^-) control field with an optical frequency of ω_C and a Rabi frequency Ω_C , and a σ^+ -polarized signal field with a frequency of ω_S . The two-photon Raman detuning is denoted as δ_R . (b) Schematic of the experimental setup. The rubidium buffer gas cell is centered within a solenoid and enclosed in magnetic shielding (not shown). The polarizing beam splitter and a quarter-wave plate are denoted as PBS and $\lambda/4$, respectively.

and does not directly depend on the width of the transmission peaks making it potentially interesting as an alternative method for measuring magnetic fields.

Here, we demonstrate a method for measuring the energy splitting between two electronic ground states in a three-level system, including the energy shift stemming from the interaction with the optical fields. We achieve this by utilizing the effect of frequency matching in light storage spectroscopy. While measurement methods exploiting the narrow two-photon resonances arising from EIT and CPT are sensitive to intensity fluctuations of all involved optical fields, we show that the observed light shift in our method is determined by the properties of the control field only. That is, we demonstrate that the retrieved optical field does not cause any additional light shifts. This has implications for light storage-based sensing schemes and quantum memories since the evolution of the underlying spin coherence during the storage period is decoupled from any intensity fluctuations of the input pulses.

2. Methods

The setup used for our experiments is similar to a previously described apparatus [23–27]. We use a 50 mm long rubidium cell containing 20 torr neon acting as a buffer gas. The temperature of the buffer gas cell is actively stabilized to approximately $T \approx 90^\circ\text{C}$ with a relative uncertainty of $\Delta T = \pm 0.02$ K. The cell is positioned in the center of a solenoid (length: $L \approx 0.34$ m; radius: $R \approx 0.05$ m) providing an approximately homogeneous magnetic bias field \vec{B}_0 aligned with the propagation direction of the optical fields to control

the splitting of the ground state Zeeman sublevels denoted as $|g_- \rangle$ and $|g_+ \rangle$ in figure 1(a). The solenoid is enclosed in three layers of μ -metal shielding in order to isolate the experiment from ambient and stray magnetic fields. An external cavity diode laser serves as a source for both the control and signal field. Its optical frequency is stabilized to the $F = 2 \rightarrow F' = 1$ transition of the rubidium D1 line near 795 nm by means of Doppler-free spectroscopy. A PBS divides the laser beam into two fields, the control and signal field, which then pass independent acousto-optic modulators to allow for precise control over their respective intensity and frequency. Subsequently, they are spatially overlapped at a second PBS and sent through a polarization maintaining single-mode optical fiber, ensuring spatial mode matching of the two fields. After exiting the fiber both fields are collimated to a beam diameter of 0.9 mm, pass through a $\lambda/4$ -plate and enter the cell with opposite circular polarisations. After traversing the buffer gas cell, the light fields' polarizations are again converted to linear by using another $\lambda/4$ -plate. This allows us to remove the control field on a PBS and to detect the signal field intensity on a photodiode. Adjustment of this $\lambda/4$ -plate in combination with the PBS allows for controlling the mixture of control and signal light reaching the photodetector.

3. Results and discussion

In initial experiments, we investigate dark resonances and the storage of light. Figure 2(a) shows the transmission of the signal beam as a function of the two-photon detuning $2\pi\delta_R = \omega_S - \omega_C - 2g_F\mu_B B/\hbar$ adjusted by controlling the frequency of the signal field at a fixed control field frequency and magnetic bias field, here chosen to be $B = B_0 \approx 0.49$ G. $\omega_S, \omega_C, g_F, \mu_B$ and \hbar denote the angular frequencies of the optical signal and control fields, the Landé g factor, the Bohr magneton, and the reduced Planck constant, respectively. With typical beam intensities (powers) of the control and the signal beam of $I_C \approx 89$ mW cm $^{-2}$ ($P_C \approx 300$ μ W) and $I_S \approx 30$ mW cm $^{-2}$ ($P_S \approx 100$ μ W), respectively, we observe a transmission window of approximately 20 kHz. In this measurement, $\delta_R = 0$ denotes the detuning where the observed transmission is maximal.

As illustrated in figure 2(b), the rubidium ensemble is irradiated with a sequence of control and signal field pulses. Firstly, the atoms are exposed to the control field only in order to prepare the population in the state $|g_- \rangle$ by means of optical pumping. Subsequently, a signal field pulse with a typical duration of approximately 1 ms is sent into the prepared medium, with its falling edge coinciding with that of the control field. After a storage period of $\tau = 5$ μ s, the control beam is turned on again to initiate the retrieval of the signal field. Figure 2(c) shows an example of such an experiment (with 50 μ s long signal pulses chosen to illustrate the timescale for reaching the steady-state) with the rapid oscillations seen both in the input and the retrieved parts of the signal being due to the optical beating with the control beam. To this end, the quarter-wave plate behind the rubidium apparatus is slightly

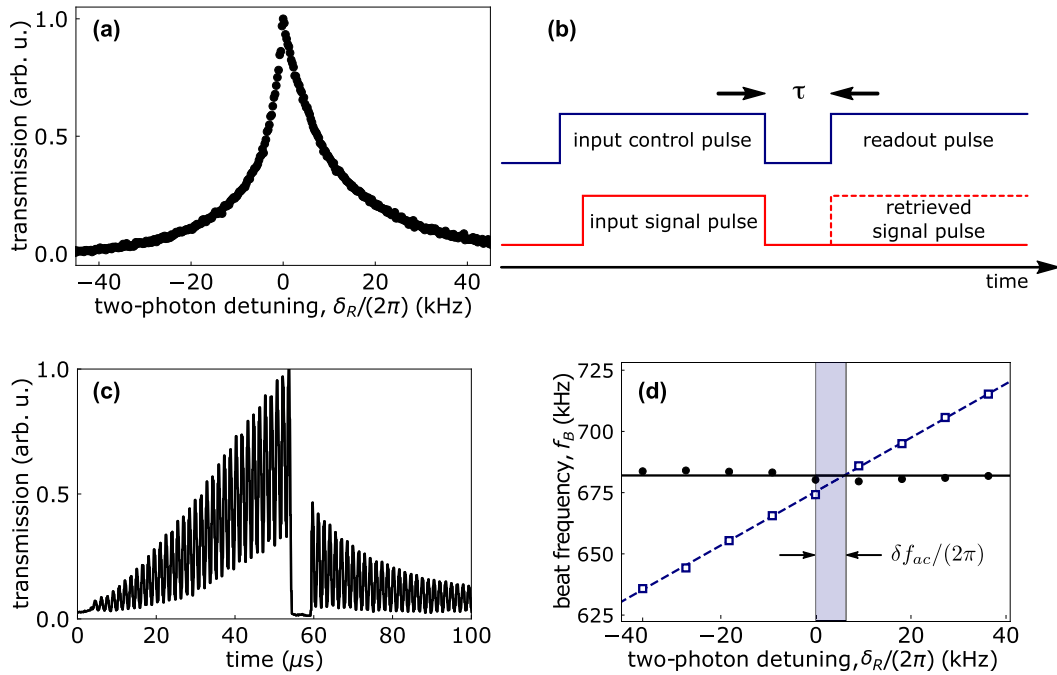


Figure 2. (a) Experimental transmission spectrum of a dark resonance with a width of approximately 20 kHz (full width at half maximum). The transmission of the signal field as a function of δ_R at a fixed magnetic bias field B_0 shows a resonance at $\delta_R = 0$. (b) Pulse sequence for light storage experiments. We start the sequence by illuminating the rubidium atoms with a control field of a chosen intensity I_C to prepare the ensemble in the state $|g_-\rangle$. The signal field with a duration of $\sim 50 \mu$ s and the control field are switched off simultaneously. In later measurements, the settling time varies with I_C and I_S , and we use 1 ms pulses to ensure that the steady-state is reached. After a storage period $\tau \approx 5 \mu$ s, the control field is turned on again, triggering the retrieval of the signal field. (c) Light storage experiment recorded with a photodiode (average over 10 consecutive realizations). The rapid oscillations arise from beating of the input (for $t < 55 \mu$ s) and the retrieved signal pulses ($t > 60 \mu$ s) with the control field. In both cases, the corresponding beating frequency f_B is extracted by fitting a sinusoidally modulated function to the data. (d) Typical result of a light storage spectroscopy experiment. At fixed B_0 , δ_R is varied within the EIT window. The extracted values of f_B for the input signal and control fields (blue hollow squares) as well as the retrieved signal and readout control fields (black circles) are shown with linear fits to the data (blue dashed line for input pulses; black solid line for readout/retrieved pulses). The beat frequency of the pulses after retrieval shows the characteristic frequency matching, i.e. f_B is constant within experimental uncertainties. The beatnotes of the input and the readout fields intersect at $\delta_R = \delta f_{ac}$ which we attribute to a differential ac Stark shift between the states $|F = 2, m_F = -2\rangle$ and $|F = 2, m_F = 0\rangle$ ($|g_-\rangle$ and $|g_+\rangle$ in figure 1(a)) induced by the control field. Here, $\delta_R = 0$ was obtained by using reduced pulse intensities and varying δ_R to maximize the retrieved beat signal. It agrees with the value in (a) within experimental uncertainties.

rotated to allow leakage of the control beam onto the photodiode. The oscillation frequency f_B of the beating signal is then determined by fitting a sinusoidally modulated function to the recorded data [23].

Under EIT conditions, at a fixed magnetic bias field, the storage experiment is repeated for different values of δ_R within the transmission window shown in figure 2(a). Figure 2(d) shows the extracted beat frequencies f_B of the control and input as well as retrieved signal fields, as a function of δ_R . While for the input pulse, f_B is determined by the difference between the control and signal fields' optical frequencies, the beat frequency of the retrieved signal remains constant within our experimental uncertainties, in agreement with the findings reported in [23, 25, 27]. This locking to the atomic resonance within the EIT window therefore acts as a spectroscopic tool for determining the two-photon resonance frequency even if the resonance condition is violated, that is for $\delta_R \neq 0$. It should be noted that despite the insensitivity to δ_R the atomic transition itself can be shifted by the interaction with light fields. To investigate this effect, we use the observed shift δf_{ac} of the intersection point away from $\delta_R = 0$ (illustrated by the vertical shaded area) as a measure for the light shift caused by the

control field. In order to obtain the approximate position of the bare atomic resonance used for calculating δf_{ac} , we initially perform this experiment with strongly reduced optical field intensities, and determine the detuning where the amplitude of the retrieved beat signal is maximal. We note that since the observed beating originates directly from the atomic coherence probed exclusively during the retrieval phase, the accuracy with which the spectral position of the Raman resonance can be determined does not directly depend on either the width or the shape of the EIT resonance, highlighting a major advantage of our measurement scheme. Dark resonances are in general asymmetric as shown exemplarily in figure 2(a) and can exhibit other significant deviations, e.g. from Lorentzian profiles in a non-trivial fashion which have to be taken into account when measuring the splitting between the ground states. Recently demonstrated methods for suppressing LAI shifts rely on the consecutive application of phase jumps during the probing period [19]. We note that in our case, the required prolonged interrogation, additional electronic stabilization as well as residual shifts due to finite ground state decoherence can be avoided, since the frequency matching is an intrinsic property of light storage itself.

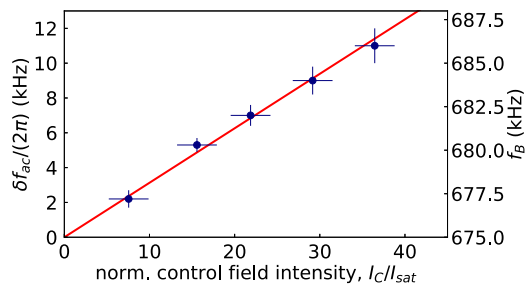


Figure 3. Light shifts measured using frequency matching in light storage experiments carried out for different intensities I_C of the control field (here normalized to the saturation intensity I_{sat}). Considering $\delta_R = 0$ from figure 2(d), the observed ac Stark shift δf_{ac} (blue data points) shows good agreement with a linear dependence on I_C as indicated by a fit with a linear function (red line). The depicted uncertainties are attributed to fluctuations of I_C and standard errors of the beating frequencies f_B (shown on the right) calculated by the fitting routine for individual values of I_C .

We now investigate the dependence of the observed shift on the intensity of the control field I_C . To this end, we repeat the series of light storage experiments as depicted in figure 2(d) for different values of I_C while keeping the magnetic bias field and the signal beam intensities constant. Figure 3 shows the result of such measurements for a signal beam intensity of $I_S = 30 \text{ mW cm}^{-2}$. We find that the ac Stark shifts observed in our experiment follow the expected linear dependence on I_C [28–31], here normalized to the effective far-detuned saturation intensity $I_{\text{sat}} \approx 4.5 \text{ mW cm}^{-2}$. We confirm this by fitting a linear function to our data, assuming that $\delta f_{\text{ac}} = 0$ for zero control field intensity. A fit with the intercept as a free parameter yields a shift consistent with zero at $I_C = 0$, confirming that the two-photon detuning corresponding to the bare atomic resonance is in agreement with the previously determined approximate value for $\delta_R = 0$. We note that, using the measured beat frequencies, the extracted intercept corresponds to the atomic transition frequency. Thus, the latter can be determined without prior knowledge of the two-photon resonance's location. The obtained results are in good agreement with the light shifts calculated assuming our simplified multi-level system and additional coupling of the control field (with an intensity averaged over the radial Gaussian beam profile) to the $5^2P_{1/2}, F = 2$ state. However, predicting the exact shift for our thermal ensembles requires more precise knowledge of numerous relevant experimental parameters [11, 28, 32]. For example, the temperature at the location of the atoms, the pressure shift, inhomogeneity of the magnetic field, impurities of the polarizations, alignment of k -vectors with the magnetic field, and the exact distribution of population between the Zeeman sublevels are known to have a direct impact on the expected light shift and have to be taken into account [32–34]. We note that in the current implementation of our scheme, no measures are taken to ensure optimal pulse shaping for light storage or retrieval [35]. In particular, due to the rectangular shape of the pulses used in our experiments, the adiabaticity condition is not necessarily fulfilled such that the population distribution in the Zeeman manifold of the $5S_{1/2}, F = 2$ state can significantly differ from the equilibrium distribution established under continuous EIT conditions.

Notwithstanding, our method provides a means for measuring the *effective differential* shift between the two ground states experienced by the atoms, including all experimental imperfections, which can be instrumental in characterizing the interaction of atomic ensembles with optical fields. As an example, in the general case of non-collinear signal and control fields intersecting at an angle α the frequency pulling is determined by the relation

$$\delta(\alpha) = \delta_R(1 - \cos(\alpha))\cos^2(\Theta)$$

[23], where Θ is the mixing angle given by

$$\tan(\Theta) = g\sqrt{N}/\Omega_C,$$

with g being the coupling strength of the signal field, N the atomic density, and Ω_C the Rabi frequency of the control field. Therefore, a comparison of the obtained shift with a theoretically predicted value for the collinear configuration, i.e. $\alpha = 0$, can be used to determine α at the location of the atomic ensemble.

Another advantage of using light storage spectroscopy for measuring light shifts is the expected insensitivity of the beat frequency with respect to the intensity of the signal field as well as its fluctuations. In the case of co-propagating signal and control fields, where complete frequency matching is expected, this can be understood intuitively in the dark state-polariton picture, where the propagation of signal field pulses is described by the quantum field [20]

$$\hat{\Psi} = \cos(\Theta)\hat{E}_S + \sin(\Theta)\sqrt{N}\hat{\sigma}_{-+}^j.$$

Here, \hat{E}_S denotes the creation operator for a photon in the signal field and $\hat{\sigma}_{-+}^j$ the spin operator representing the change of the state of the j th atom from $|g_{-}\rangle$ to $|g_{+}\rangle$, respectively. As a fundamental consequence of the light storage process, no external signal fields are present during the storage period ($\Theta = \pi/2$), and all subsequently retrieved photons in the signal beam mode are created by the interaction of the control (read-out) field with the prepared atomic spin-wave component of the polariton.

We now test the prediction that the total light shift is insensitive to the intensity of the signal field by performing light storage experiments as discussed in the context of figure 3, but for different signal field intensities while the control field intensity is kept constant at $I_C = 89 \text{ mW cm}^{-2}$. Figure 4 shows such beat frequency measurements carried out again at a fixed magnetic bias field. In the case of signal field intensities comparable to values used in the previous measurement, we obtain $\delta f_{\text{ac}}/(2\pi) \approx 7 \text{ kHz}$, in agreement with the result shown in figure 3. However, for varied I_S , we now observe that f_B remains constant within our experimental uncertainty. That is, a linear fit to the data yields a slope comparable to the corresponding standard error and approximately 30 times smaller than the value obtained for the case of varied control field intensity after accounting for the different Clebsch–Gordan coefficients of the respective optical transitions. Moreover, for signal field intensities below the point where the approximation of weak signal fields breaks down, i.e. $I_S \approx I_C$, as indicated by the shaded area, our analysis reveals a slope consistent

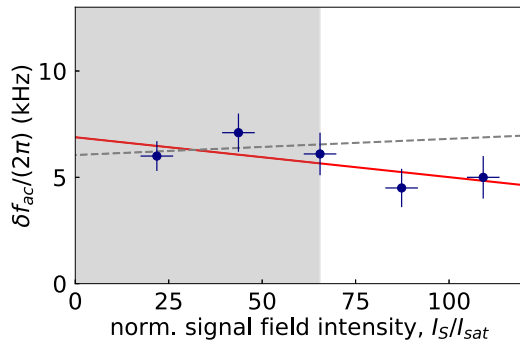


Figure 4. Light shift as a function of the normalized input signal field intensity. For a fixed magnetic bias field and control field intensity, the storage experiment is performed for different I_S . A linear fit to all extracted frequency shifts (red solid line) and to the data within the grey shaded area indicating the range $I_S \leq I_C$ (grey dashed line), yields a slope comparable to the corresponding standard error and a slope that is consistent with zero, respectively.

with zero. In the regime where I_S exceeds I_C , a residual non-vanishing slope could be the result of non-trivial population dynamics in the ground state manifold occurring during the preparation phase, leading to a distribution encountered upon readout that is no longer confined to the magnetic quantum numbers $m_F = -2$ and $m_F = 0$ as assumed for the idealized Λ system. In addition, due to strongly enhanced four-wave mixing observed in EIT media [7, 36], additional optical fields can be generated during the propagation of the signal field pulses, which in turn would manifest themselves as sidebands in the beating signal. Since our current analysis only takes into account a single spectral component of the beatnote, the presence of such sidebands can lead to systematic deviations that become more pronounced with increasing signal field intensity. Nonetheless, this finding is in clear contrast to the demonstrated statistically significant linear dependence of the light shift with respect to the intensity of the control field, confirming that the energetic shift in our light-storage scheme is predominantly or solely caused by the control field. Consequently, extending light-storage spectroscopy to tripod-type systems comprising four electronic levels coupled by two signal fields and one control field may allow to measure the energetic splitting between the outer electronic ground states [25] while effectively avoiding the impact of light shifts. This is a consequence of the signal being derived from the beat note between the two signal fields whose respective one-photon detunings, upon retrieval initiated by a common control field, are shifted by the same amount. Along similar lines, if the signal fields are chosen to couple magnetically sensitive ground states, e.g. different Zeeman sublevels within a hyperfine manifold, the same methods could be applied to measure either magnetic fields [25] or magnetic field gradients [26] with improved precision.

4. Conclusion

To summarize, we have shown that light-storage spectroscopy can be used to measure control field-induced differential light shifts between electronic ground states while at the same

time measuring their energetic splitting. The method is readily applicable to all conventional CPT-based light shift measurement schemes using continuous exposure to signal and control fields, even for strongly asymmetric transmission profiles, since it only requires minor modifications regarding the capability to operate the optical fields in a pulsed fashion. Lastly, we show that the light shift is independent of the intensity of the signal field within our experimental uncertainties, potentially allowing to improve the precision of clocks, magnetometers or magnetogradiometers exploiting CPT or EIT in suitable three-level systems. To this end, one might exploit the technical compatibility of our LSS method with most CPT-based schemes routinely employing modulation of optical intensities, frequencies or phases, such that many of the established methods for mitigating the light shifts [14–18] can be applied during the readout (retrieval) phase in our measurements. In the described three-level system, this should lead to a similar suppression of the residual control field-induced light shifts, while the impact of the signal fields, whose intensities are typically of the same order of magnitude, as well as, e.g. LAI shifts are intrinsically suppressed without the otherwise required overhead in terms of sequence complexity, prolonged interrogation times and electronic stabilization [19]. Lastly, we discuss how the influence of ac Stark shifts in such precision measurements might be suppressed by using previously demonstrated extensions to tripod-type four-level configurations. It will be interesting to test these predictions in future experiments featuring a more refined control of the system, ideally carried out with ultracold atomic ensembles allowing for drastically improved magnetic field homogeneity and eliminating buffer gas shifts, and where many relevant parameters can be determined with very high precision. For instance, ion Coulomb crystals are a system holding great promise for improving the coherence time and light storage efficiency required for precision measurements [37] owing to favourable properties such as intrinsically suppressed collisional decoherence, while potential detrimental effects stemming from the presence of micromotion [12, 38] might be avoided by using optical trapping techniques [39–43].




Acknowledgments

The authors acknowledge financial support from the University of Freiburg, Innovationsfonds Forschung Project No. 2100189901.

Data availability statement

The data that support the findings of this study are available upon reasonable request from the authors.

ORCID iDs

D Palani  <https://orcid.org/0000-0002-0938-9273>
 D Hoenig  <https://orcid.org/0000-0003-2007-4691>
 L Karpa  <https://orcid.org/0000-0003-2652-5043>

References

- [1] Alzetta G, Gozzini A, Moi L and Orriols G 1976 An experimental method for the observation of r.f. transitions and laser beat resonances in oriented Na vapour *Il Nuovo Cimento B* **36** 5–20
- [2] Arimondo E 1996 Coherent population trapping in laser spectroscopy *Progress in Optics* vol 35 (Amsterdam: Elsevier) pp 257–354
- [3] Harris S E, Field J E and Imamoglu A 1990 Nonlinear optical processes using electromagnetically induced transparency *Phys. Rev. Lett.* **64** 1107–10
- [4] Fleischhauer M, Imamoglu A and Marangos J P 2005 Electromagnetically induced transparency: optics in coherent media *Rev. Mod. Phys.* **77** 633–73
- [5] Brandt S, Nagel A, Wynands R and Meschede D 1997 Buffer-gas-induced linewidth reduction of coherent dark resonances to below 50 Hz *Phys. Rev. A* **56** R1063–6
- [6] Hau L V, Harris S E, Dutton Z and Behroozi C H 1999 Light speed reduction to 17 metres per second in an ultracold atomic gas *Nature* **397** 594–8
- [7] Kash M M, Sautenkov V A, Zibrov A S, Hollberg L, Welch G R, Lukin M D, Rostovtsev Y, Fry E S and Scully M O 1999 Ultraslow group velocity and enhanced nonlinear optical effects in a coherently driven hot atomic gas *Phys. Rev. Lett.* **82** 5229–32
- [8] Budker D, Kimball D F, Rochester S M and Yashchuk V V 1999 Nonlinear magneto-optics and reduced group velocity of light in atomic vapor with slow ground state relaxation *Phys. Rev. Lett.* **83** 1767–70
- [9] Scully M O and Fleischhauer M 1992 High-sensitivity magnetometer based on index-enhanced media *Phys. Rev. Lett.* **69** 1360–3
- [10] Katsoprinakis G, Petrosyan D and Kominis I K 2006 High frequency atomic magnetometer by use of electromagnetically induced transparency *Phys. Rev. Lett.* **97** 230801
- [11] Vanier J 2005 Atomic clocks based on coherent population trapping: a review *Appl. Phys. B* **81** 421–42
- [12] Ludlow A D, Boyd M M, Ye J, Peik E and Schmidt P O 2015 Optical atomic clocks *Rev. Mod. Phys.* **87** 637–701
- [13] Zanon-Willette T *et al* 2018 Composite laser-pulses spectroscopy for high-accuracy optical clocks: a review of recent progress and perspectives *Rep. Prog. Phys.* **81** 094401
- [14] Abdel Hafiz M, Coget G, Petersen M, Rocher C, Guérandel S, Zanon-Willette T, de Clercq E and Boudot R 2018 Toward a high-stability coherent population trapping Cs vapor-cell atomic clock using autobalanced Ramsey spectroscopy *Phys. Rev. Appl.* **9** 064002
- [15] Abdel Hafiz M, Coget G, Petersen M, Calosso C E, Guérandel S, de Clercq E and Boudot R 2018 Symmetric autobalanced Ramsey interrogation for high-performance coherent-population-trapping vapor-cell atomic clock *Appl. Phys. Lett.* **112** 244102
- [16] Abdel Hafiz M *et al* 2020 Protocol for light-shift compensation in a continuous-wave microcell atomic clock *Phys. Rev. Appl.* **14** 034015
- [17] Shuker M, Pollock J W, Boudot R, Yudin V I, Taichenachev A V, Kitching J and Donley E A 2019 Reduction of light shifts in Ramsey spectroscopy with a combined error signal *Appl. Phys. Lett.* **114** 141106
- [18] Shuker M, Pollock J W, Boudot R, Yudin V I, Taichenachev A V, Kitching J and Donley E A 2019 Ramsey spectroscopy with displaced frequency jumps *Phys. Rev. Lett.* **122** 113601
- [19] Yu Basalaev M, Yudin V I, Taichenachev A V, Vaskovskaya M I, Chuchelov D S, Zibrov S A, Vassiliev V V and Velichansky V L 2020 Dynamic continuous-wave spectroscopy of coherent population trapping at phase-jump modulation *Phys. Rev. Appl.* **13** 034060
- [20] Fleischhauer M and Lukin M D 2000 Dark-state polaritons in electromagnetically induced transparency *Phys. Rev. Lett.* **84** 5094–7
- [21] Liu C, Dutton Z, Behroozi C H and Hau L V 2001 Observation of coherent optical information storage in an atomic medium using halted light pulses *Nature* **409** 490–3
- [22] Phillips D F, Fleischhauer A, Mair A, Walsworth R L and Lukin M D 2001 Storage of light in atomic vapor *Phys. Rev. Lett.* **86** 783–6
- [23] Karpa L, Nikoghosyan G, Vewinger F, Fleischhauer M and Weitz M 2009 Frequency matching in light-storage spectroscopy of atomic Raman transitions *Phys. Rev. Lett.* **103** 093601
- [24] Karpa L and Weitz M 2008 Slow light in inhomogeneous and transverse fields *New J. Phys.* **10** 045015
- [25] Karpa L, Vewinger F and Weitz M 2008 Resonance beating of light stored using atomic spinor polaritons *Phys. Rev. Lett.* **101** 170406
- [26] Karpa L and Weitz M 2010 Nondispersive optics using storage of light *Phys. Rev. A* **81** 041802
- [27] Djokic V, Enzian G, Frank V and Weitz M 2015 Resonance retrieval of stored coherence in an rf-optical double-resonance experiment *Phys. Rev. A* **92** 063802
- [28] Arditi M and Carver T R 1961 Pressure, light, and temperature shifts in optical detection of 0–0 hyperfine resonance of alkali metals *Phys. Rev.* **124** 800–9
- [29] Dalibard J and Cohen-Tannoudji C 1989 Laser cooling below the Doppler limit by polarization gradients: simple theoretical models *J. Opt. Soc. Am. B* **6** 2023
- [30] Miletić D, Affolderbach C, Hasegawa M, Boudot R, Gorecki C and Mileti G 2012 Ac Stark-shift in CPT-based Cs miniature atomic clocks *Appl. Phys. B* **109** 89–97
- [31] Metcalf H and van der Straten P 1999 *Laser Cooling and Trapping* (Berlin: Springer)
- [32] Wynands R and Nagel A 1999 Precision spectroscopy with coherent dark states *Appl. Phys. B: Lasers Opt.* **68** 1–25
- [33] Steck D A 2008 Rubidium 87 D line data <http://steck.us/alkalidata>, revision 2.0.1
- [34] Pollock J W, Yudin V I, Shuker M, Basalaev M Y, Taichenachev A V, Liu X, Kitching J and Donley E A 2018 Ac Stark shifts of dark resonances probed with Ramsey spectroscopy *Phys. Rev. A* **98** 053424
- [35] Novikova I, Gorshkov A V, Phillips D F, Sørensen A S, Lukin M D and Walsworth R L 2007 Optimal control of light pulse storage and retrieval *Phys. Rev. Lett.* **98** 243602
- [36] Camacho R M, Vudyaasetu P K and Howell J C 2009 Four-wave-mixing stopped light in hot atomic rubidium vapour *Nat. Photonics* **3** 103–6
- [37] Albert M, Dantan A and Drewsen M 2011 Cavity electromagnetically induced transparency and all-optical switching using ion Coulomb crystals *Nat. Photonics* **5** 633–6
- [38] Cirac J I, Garay L J, Blatt R, Parkins A S and Zoller P 1994 Laser cooling of trapped ions: the influence of micromotion *Phys. Rev. A* **49** 421–32
- [39] Lambrecht A, Schmidt J, Weckesser P, Debatin M, Karpa L and Schaetz T 2017 Long lifetimes and effective isolation of ions in optical and electrostatic traps *Nat. Photonics* **11** 704–7
- [40] Schaetz T 2017 Trapping ions and atoms optically *J. Phys. B: At. Mol. Opt. Phys.* **50** 102001
- [41] Schmidt J, Lambrecht A, Weckesser P, Debatin M, Karpa L and Schaetz T 2018 Optical trapping of ion Coulomb crystals *Phys. Rev. X* **8** 021028
- [42] Karpa L 2019 *Trapping Single Ions and Coulomb Crystals with Light Fields (Springer Briefs in Physics)* (Cham: Springer)
- [43] Schmidt J, Weckesser P, Thielemann F, Schaetz T and Karpa L 2020 Optical traps for sympathetic cooling of ions with ultracold neutral atoms *Phys. Rev. Lett.* **124** 053402